

Vibrations of closed-shell Lennard-Jones icosahedral and cuboctahedral clusters and their effect on the cluster ground-state energy

Antonio Šiber*

Institute of Physics, P.O. Box 304, 10001 Zagreb, Croatia

(Received 1 March 2004; revised manuscript received 3 May 2004; published 18 August 2004)

Vibrational spectra of closed shell Lennard-Jones icosahedral and cuboctahedral clusters are calculated for shell numbers between 2 and 9. Evolution of the vibrational density of states with the cluster shell number is examined and differences between icosahedral and cuboctahedral clusters described. This enabled a quantum calculation of ground state energies of the clusters in the quasiharmonic approximation and a comparison of the differences between the two types of clusters. It is demonstrated that in the quantum treatment, the closed shell icosahedral clusters binding energies differ from those of cuboctahedral clusters more than is the case in classical treatment.

DOI: 10.1103/PhysRevB.70.075407

PACS number(s): 61.46.+w, 63.22.+m, 36.40.Mr

I. INTRODUCTION

The interest of the condensed matter community in cluster physics has been recently revived due to exciting technological possibilities offered by new materials in which clusters play the role of basic “building blocks” (see, e.g., Ref. 1). Theoretical investigations of model clusters, i.e., assemblies of particles interacting via binary (mostly Lennard-Jones) potential has a long history.^{2–16} Most studies performed so far have concentrated on the search of the most stable configuration of N particles. Typically, total potential energy of a cluster is written as a sum over binary interactions of all pairs of particles within the cluster. Then, a search for a set of coordinates (or configuration of the cluster) which minimize the potential energy is performed. Depending on the number of particles within a cluster, very different cluster shapes can be obtained following this procedure.^{9,14} The approach just sketched can require formidable numerical optimization procedures.¹¹ However, it is completely classical since it produces an absolute minimum in the potential energy, rather than the energy of a ground quantum state of the system which must be smaller in absolute value. The difference between the two values is the (quantum) zero-point energy of the cluster.

The clusters investigated in this article are known as closed shell clusters. These appear for “magic values” of N , and the specific sequence to be investigated here is $N = 13, 55, 147, 309, 561, 923, \dots$. The characteristic sequence of “magic” numbers has also been observed experimentally (see, e.g., Ref. 17). Closed shell clusters of interest to the present article appear in two configurations, icosahedral and cuboctahedral (see Fig. 1). These clusters can be thought of as being assembled by adding closed “shells” of atoms to a single atom located at the origin, i.e., the center of the cluster. The thus “assembled” structure can be characterized with the maximum shell number n (see Fig. 1). The two types of clusters have quite different geometries, but their common feature is that they have the same number of atoms for the given maximum shell number n .⁷ This is a very convenient feature which enables a direct comparison of the various physical properties of such clusters.^{5–13} Cuboctahedral clus-

ters can also be visualized as pieces of a crystal with face-centered-cubic (FCC) packing. An FCC crystal can be obtained from cuboctahedral clusters in the limit of infinite shell number. The same is not true for icosahedral clusters which are therefore “noncrystal.”⁷ Closed shell icosahedral configuration has been shown to have lower total potential energy for clusters smaller than about 9000 particles.⁵ The actual number of particles (or the shell number)⁵ above which cuboctahedral clusters have lower potential energy has been a subject of debate (see, e.g., Refs. 5, 10, and 18). This is not important for the purpose of this article since I am going to consider relatively small clusters (up to nine shells or 2869 atoms) for which icosahedral configuration is a classically preferred one. A plausible reason for the fact that the closed shell icosahedral (CSIC) configuration is classically more stable from the closed shell cuboctahedral (CSFCC) configuration is that the arrangement of particles which are on the cluster surface is “tighter” in the CSIC than in the CSFCC ordering of the cluster (see Fig. 1).

A word of caution is in order here: It is well known that the closed shell cuboctahedral clusters are not the energeti-

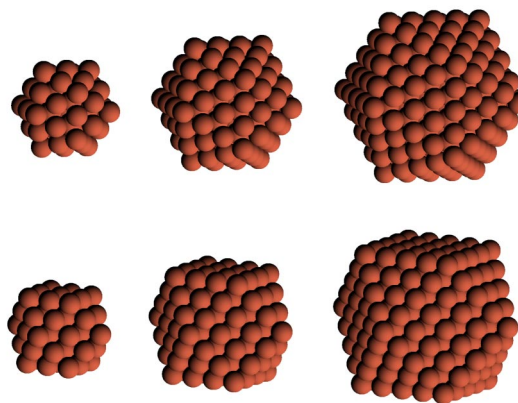


FIG. 1. Closed shell icosahedral (CSIC, top panel) and cuboctahedral (CSFCC, bottom panel) Lennard-Jones clusters in their minimum potential energy configuration for maximum shell numbers $n=2, 3$, and 4 (from left to right).

cally most favored crystalline clusters, since they expose relatively large, poorly coordinated FCC(100) surface area¹⁹ (for example, the most stable configuration for 38 atoms interacting via Lennard-Jones binary potentials is truncated octahedron^{14,16}). The fact that the closed-shell configurations of icosahedral and cuboctahedral clusters have the same number of atoms is the primary reason for the choice of CSFCC clusters as a subject of this study. This enables one a direct and unambiguous comparison of various properties of clusters with different symmetries. Alternatively, the approach of this article could be easily applied for comparison of clusters with different number of atoms, however, in this case one would be restricted to a comparison of quantities *per particle*.

The aim of this article is twofold. First, a detailed microscopic calculation of cluster vibrations shall be performed, depending on the closed-shell cluster size. It is of interest to see whether the different cluster geometries reflect themselves in the cluster vibrational properties. The differences in vibrational properties could be exploited to discriminate between the different cluster geometries. Some early studies²⁻⁴ have dealt with the vibrational frequency spectra of clusters, but these studies were limited to quite small clusters and there were no attempts to compare the vibrational spectra pertaining to clusters with the different symmetries. The results should also be relevant to the studies of vibrations in nanoparticles deposited on substrates.²⁰ The second aim is to reexamine the cluster stability from the point of quantum mechanics, i.e., to investigate the differences between the CSIC and CSFCC clusters with respect to their quantum ground state energy and temperature dependent vibrational entropy. The quantum approach is quite easy in the case in which the cluster dynamics can be adequately represented by harmonic vibrations, but it should be kept in mind that such treatment is adequate only for sufficiently low temperatures. This is the region of temperatures that is of interest to this article. There are several points that come to mind regarding the second aim. First, one could assume that the fact that the surfaces of CSFCC clusters are less densely packed implies that their characteristic vibrations will be “softer,” i.e., of lower frequency. Thus, zero-point energy of CSFCC clusters could be expected to be smaller, and the shift of the ground state energy from absolute minimum of the potential energy lesser than in CSIC clusters. This would suggest that quantum ground state energy may even be larger (in absolute units) in CSFCC clusters, which would promote them to thermodynamically preferred configurations of N atoms at zero temperature, $T=0$ K. Second, even if the zero-point energy is not sufficiently different in the two cases, in order to find the thermodynamically preferred configuration at finite temperature one should minimize free energy of the system. As the cluster free energy depends on the features of the cluster vibrational spectrum and temperature, it may happen that at some finite temperature, T_c , the free energy of the CSFCC configuration becomes smaller than the free energy of the CSIC configuration, even if its ground state, binding energy was smaller than in the CSIC configuration. Third, as vibrational frequencies depend on the mass of particles in the cluster, M , quantum effects and thermodynamical considerations must be mass dependent. Classically, the cluster sta-

bility considerations depend only on the binary interaction potential. Thus, any two clusters composed of different isotopes of the same element will always have the same configuration. Obviously, this needs not be the case in a quantum treatment and quantum effects are going to be larger for clusters composed of lighter particles. This article aims at examining the three points mentioned above. The results of the article are not directly applicable to real clusters, although the model of the cluster adopted could be used to describe noble gas clusters and could serve as a point of departure for setting up more complex interaction models.^{13,15} There are some reservations, however, since it is known that the form of the binary potential employed in calculation can influence the cluster optimal shape and its dynamical properties.^{8,13} Additionally, the results of this article cannot be directly applied to discuss the energy crossover between the IC and FCC clusters depending on the number of atoms,¹³ since the type of the FCC clusters chosen in this study is not the most energetically favored one. Nevertheless, the results obtained should be useful for a general insight in the quantum effects on the cluster ground state energy.

The article is organized as follows: In Sec. II, I shall briefly describe the adopted theoretical approach (quantum quasiharmonic approximation). Section III deals with the model clusters in which the particles interact via Lennard-Jones binary potentials. Vibrational spectra of CSIC and CSFCC clusters are calculated for shell numbers between three (147 atoms) and nine (2869 atoms). The effects of mass and temperature on the Helmholtz free energy of clusters are considered on the example of clusters of Ne, Ar, and Xe atoms. Section IV summarizes and concludes the article.

II. PREREQUISITES FOR THE CALCULATION OF THE VIBRATIONS AND VIBRATIONAL FREE ENERGY OF CLUSTERS

The dynamical behavior of a cluster is described by a set of coordinates $\{\mathbf{r}_1, \mathbf{r}_2, \dots, \mathbf{r}_N\}$ which are treated as time dependent variables. The particles within the cluster are assumed to interact via a binary potential, v , which depends only on their relative positions, i.e., $v(\mathbf{r}_i, \mathbf{r}_j) = v(|\mathbf{r}_i - \mathbf{r}_j|)$. The total potential energy of the cluster, V_p is assumed to be given by a summation of binary interactions over all the pairs of particles in the cluster,

$$V_p(\{\mathbf{r}_1, \dots, \mathbf{r}_N\}) = \sum_{i>j} v(|\mathbf{r}_i - \mathbf{r}_j|), \quad (1)$$

where the dependence of the potential energy on the cluster configuration has been emphasized. The configuration of a cluster which minimizes the potential energy function can be denoted by a set of coordinates $\{\mathbf{r}_1^0, \mathbf{r}_2^0, \dots, \mathbf{r}_N^0\}$ which denote mean, static positions of the N particles within the cluster. Assuming that $\mathbf{u}_i = \mathbf{r}_i - \mathbf{r}_i^0$; $|\mathbf{u}_i| \ll |\mathbf{r}_i^0 - \mathbf{r}_j^0|$, $\forall i, j \in \{1, \dots, N\}$, i.e., that the displacements of particles from their equilibrium positions are small, one can expand the total potential energy of the cluster in the Taylor series up to the second order as

$$V_p(\{\mathbf{r}_1, \dots, \mathbf{r}_N\}) = V_p(\{\mathbf{r}_1^0, \dots, \mathbf{r}_N^0\}) + \frac{1}{2} \sum_{i,j} \sum_{\alpha,\beta} u_i^\alpha u_j^\beta \left(\frac{\partial^2 V_p}{\partial r_i^\alpha \partial r_j^\beta} \right)_0, \quad (2)$$

where α and β denote the Cartesian components (x , y , and z) of the vectors. The first derivatives of V_p with respect to atom coordinates are assumed to vanish, i.e., the cluster is assumed to be in a minimum potential energy configuration. This is the well known harmonic approximation and it serves as a starting point for the calculation of the cluster normal modes of vibration,²¹ i.e., a set of linear combinations of $\{\mathbf{u}_1, \dots, \mathbf{u}_N\}$ variables (or eigenmodes), each of which corresponds to a vibration of the system with a single frequency.²² The Hamiltonian of the problem when written in terms of normal mode coordinates represents a set of independent harmonic oscillators whose both quantum and classical dynamics are well known. There are $3N-6$ such oscillators with characteristic frequencies ω_p , $p=1, \dots, 3N-6$. Six degrees of freedom that do not represent vibrations are three rotations and three translations of the whole system.

Once a set of eigenfrequencies is calculated, one can proceed to calculate the Helmholtz free energy of the cluster, F , which is given by

$$F = -k_B T \ln Z, \quad (3)$$

where k_B is the Boltzmann constant, T is temperature, and Z is the quantum partition function of a system of $3N-6$ independent oscillators. In terms of the eigenmode frequencies, one can write²¹

$$F = V_p^0 + \sum_{p=1}^{3N-6} \frac{\hbar \omega_p}{2} + k_B T \sum_{p=1}^{3N-6} \ln \left[1 - \exp\left(-\frac{\hbar \omega_p}{k_B T}\right) \right], \quad (4)$$

where

$$V_p^0 = V_p(\{\mathbf{r}_1^0, \dots, \mathbf{r}_N^0\}), \quad (5)$$

is the minimum of classical potential energy of the cluster (classical ground state energy), and \hbar is the reduced Planck constant. The sum of the first two terms in Eq. (4) represents the quantum ground state energy of the cluster, E_0 , calculated in the harmonic approximation.

At constant temperature, the state which represents thermodynamical equilibrium of the system is the one which minimizes the Helmholtz free energy.²³ Note that even at zero temperature, the cluster free energy has a quantum, zero-point energy contribution [second term in Eq. (4)], in agreement with the ideas put forth in the Introduction. Thus, even at zero temperature, the thermodynamical equilibrium state of the cluster need not be the same as the state which minimizes the classical potential energy of the cluster.¹² This of course depends on the nature of particles in the system, their mass in particular as is known from the studies of systems of He atoms.²⁴

III. POTENTIAL ENERGY MINIMA, VIBRATIONAL SPECTRA, AND ZERO-POINT ENERGIES OF LENNARD-JONES CSIC AND CSFCC CLUSTERS

In order to perform a normal vibrational mode calculation, one first has to find the set of coordinates $\{\mathbf{r}_1^0, \mathbf{r}_2^0, \dots, \mathbf{r}_N^0\}$ which make the functional V_p stationary in the $3N$ -dimensional configurational space. If the normal mode calculation were performed in a nonstationary configuration, some of the normal mode frequencies would turn out imaginary. This would signify the instability of the cluster structure.²¹

The atoms were assumed to interact via binary Lennard-Jones 6-12 potentials,

$$v(|\mathbf{r}_i - \mathbf{r}_j|) \equiv v(r) = 4\epsilon \left[\left(\frac{\sigma}{r} \right)^{12} - \left(\frac{\sigma}{r} \right)^6 \right], \quad (6)$$

and were initially arranged in a configuration which has the symmetry of either cuboctahedral or icosahedral cluster with the nearest-neighbor atom distances set close to the Lennard-Jones range parameter σ . The thus obtained initial configuration was then allowed to relax to a configuration in which the forces acting on each of the atoms in the cluster were smaller than some predefined and arbitrarily small absolute force. To obtain the relaxed configuration, each of the atoms in the cluster was displaced a certain distance in the direction of the total force acting on it. This was repeated until the absolute value of the force averaged over all cluster atoms dropped below predefined force f_c . In each step of this iterative procedure, the lengths of vectors the atoms were moved along were reduced or enlarged, depending on the vectorial characters of forces in a given and preceding step acting on a particular atom. Apparently similar relaxation algorithms were used in Refs. 2-4, 6. The value of f_c used in the calculations presented below was $2.0 \times 10^{-13} \epsilon/\sigma$. It was observed that the $n=2$ CSFCC configuration is unstable and transforms into $n=2$ CSIC configuration. This is a fact that is well known in the literature.^{3,4,14,25} The comparison of various properties of CSFCC and CSIC clusters was thus made for n between 3 and 9, although the properties of the $n=2$ CSIC cluster were also considered.

The classical potential energies of the clusters, V_p^0 obtained using the procedure explained in the previous paragraph are displayed in Table I for closed-shell clusters with maximum shell number n . These energies depend only on ϵ , and this was used as a scale for V_p^0 . The minimum nearest neighbor distance within the cluster, $r_{\min} = \min\{|\mathbf{r}_i - \mathbf{r}_j|\}, i, j = 1, \dots, N, i \neq j$, is also displayed. The values of V_p^0 are equal to those obtained in Ref. 5 in the first six significant decimal places. This confirms the validity of the relaxation algorithm used in this work. The minimal nearest neighbor distance found in clusters is always between the central atom and one of the atoms in the first cuboctahedral or icosahedral shell. It is of interest to note that the nearest neighbor distance in Lennard-Jones 6-12 FCC crystal is 1.09017σ .²¹

When the equilibrium configuration was obtained, the force-constants [second derivatives of the binary potential function, see Eq. (2)] acting between all pairs of atoms within the cluster were calculated, the dynamical vibrational

TABLE I. Classical potential energies (V_p^0) in units of ϵ and minimum nearest neighbor distances (r_{\min}) in units of σ of Lennard-Jones icosahedral and cuboctahedral closed-shell clusters. The maximum cluster shell number is denoted by n , and total number of atoms in the cluster by N .

n	N	Icosahedral, CSIC		Cuboctahedral, CSFCC	
		V_p^0 (ϵ)	r_{\min} (σ)	V_p^0 (ϵ)	r_{\min} (σ)
2	55	-279.2485	1.05045		
3	147	-876.4612	1.03548	-854.3766	1.09093
4	309	-2007.219	1.02596	-1971.561	1.08998
5	561	-3842.394	1.01904	-3792.097	1.08929
6	923	-6552.723	1.01361	-6488.217	1.08894
7	1415	-10308.89	1.00914	-10232.14	1.08872
8	2057	-15281.55	1.00535	-15196.07	1.08842
9	2869	-21641.35	1.00205	-21552.22	1.08821

matrix was set up and its diagonalization performed in order to obtain eigenmode frequencies and polarization vectors.²¹ The frequencies obtained in such a way depend on the atom mass, M , and on the Lennard-Jones potential parameters, but only through their combination, $\omega_0 \equiv \sqrt{\epsilon/(M\sigma^2)}$.²⁶ This combination of parameters was used as a universal frequency scale.

Figures 2 and 3 display the vibrational densities of states per atom, $\rho(\omega)/N$ of CSIC and CSFCC clusters, respectively, as a function of maximum cluster shell number. The vibrational density of states was calculated as

$$\rho(\omega) = \sum_{p=1}^{3N-6} \delta(\omega - \omega_p). \quad (7)$$

For the sake of easier visualization, the δ -functions in the above equation were represented by normalized Gaussians with a width parameter of $0.02 \omega_0$. The phonon density of states per atom of the FCC Lennard-Jones 6-12 crystal is displayed in the bottom panels of Figs. 2 and 3 for comparison. The phonon density of states for the FCC crystal was calculated by numerical sampling of the three-dimensional inverse (wave vector) space in 3 000 000 randomly distributed points.

One can immediately note quite different scales on x -axes in Figs. 2 and 3. This is due to the fact that the vibrational spectra of CSIC clusters contain a high-frequency tail which is not present in the CSFCC case. For example, the maximum frequency of $n=3$ CSIC cluster is $\omega_{\max}=37.20\omega_0$, while in $n=3$ CSFCC cluster it amounts to $\omega_{\max}=25.96\omega_0$. The reason for such a large difference can be found in the data presented in Table I. From the inspection of minimum nearest-neighbor distances, one can conclude that the CSIC clusters are more tightly packed and that some of the neighbors are in a repulsive region of their binary interaction potential [the minimum of the Lennard-Jones 6-12 binary potential is at $r=1.122\sigma$ (Ref. 27)]. This especially applies to the central cluster atom which is very tightly surrounded by the atoms in the first icosahedral shell (see Table I). The

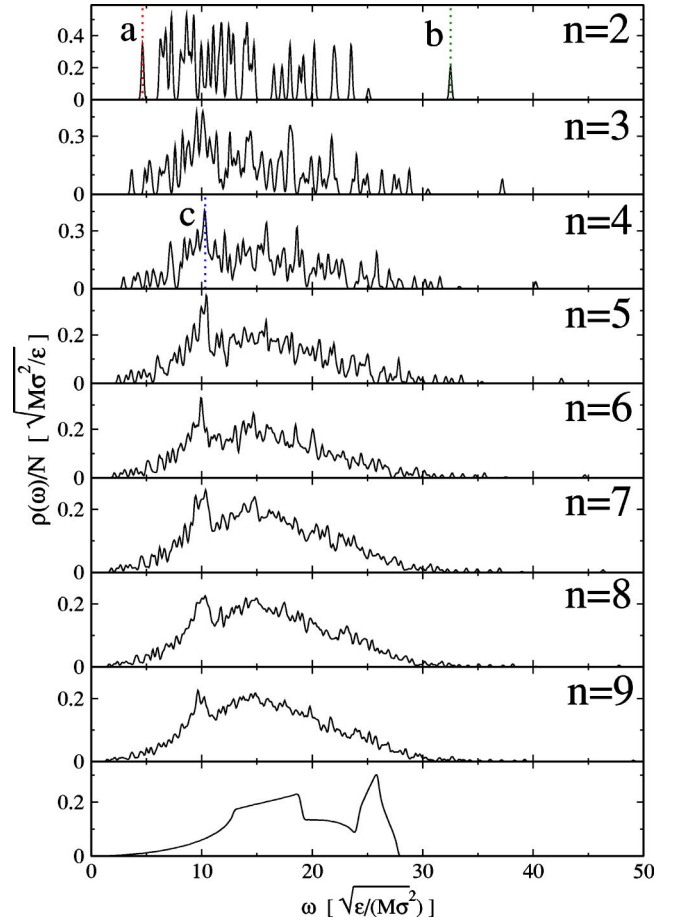


FIG. 2. Vibrational densities of states of CSIC clusters as a function of maximum shell number, $n=2, \dots, 9$. The vibrational density of states of Lennard-Jones FCC crystal is displayed in the bottom panel for comparison.

modes that dominantly represent relative motion of such atoms have therefore quite high frequencies. To substantiate this claim, I have plotted in Fig. 4 the eigenvectors (or displacement patterns) of some of the characteristic modes pertaining to CSIC clusters. The displacement pattern of the highest frequency mode of $n=2$ CSIC cluster is represented in panel (b) of Fig. 4. It can be seen that in this mode the motion of the central atom dominates the displacement pattern. Atoms in the first shell also slightly move, so that the total linear and angular momenta of the mode equal to zero, as they should. An analogous mode in the $n=3$ CSFCC cluster is depicted in panel (b) of Fig. 5. Again, the highest frequency mode is such that the central atom performs motion with the largest amplitude of all atoms in the cluster. The displacement patterns of the lowest frequency modes in $n=2$ CSIC and $n=3$ CSFCC clusters are depicted in panels (a) of Figs. 4 and 5, respectively. It is of interest to note that the displacement pattern of the lowest frequency mode in $n=2$ CSIC cluster is a sort of a “twisting” mode in which two halves of the cluster perform motions which look almost like the rotations around the same axis, but in opposite directions for the “upper” and “lower” halves of the cluster.

Further inspection of the vibrational densities of states reveals significant differences between CSFCC and CSIC

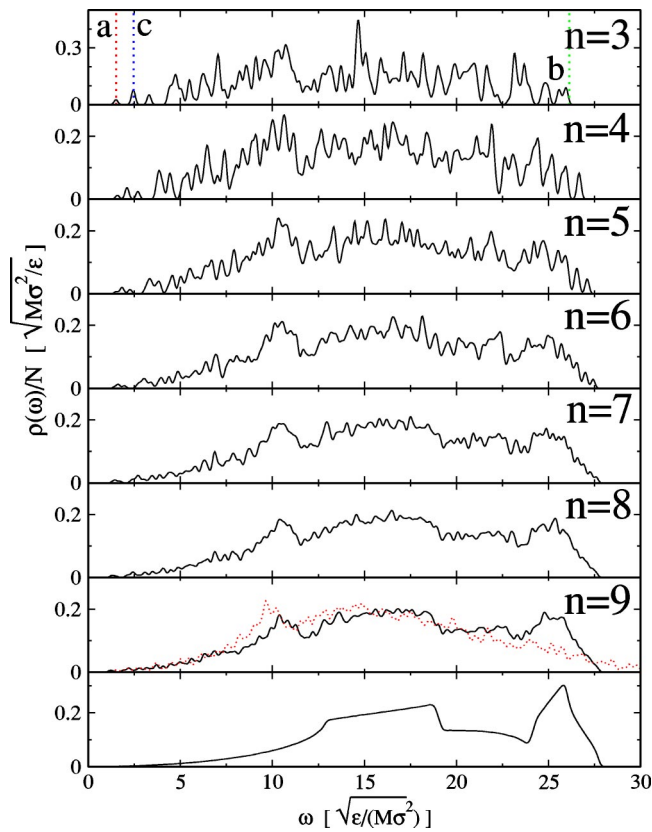


FIG. 3. Vibrational densities of states of CSFCC clusters as a function of maximum shell number, $n=3, \dots, 9$. The vibrational density of states of Lennard-Jones FCC crystal is displayed in the bottom panel for comparison. In panel denoted by $n=9$, the vibrational density of $n=9$ CSIC cluster is also displayed and denoted by a dotted line.

clusters even in the region of frequencies which contains the highest percentage of all vibrational modes (i.e., disregarding the high-frequency tail of the density of states in CSIC case). While $\rho(\omega)$ of CSFCC clusters obviously tends to the bulk (crystal) limit (except for the characteristic features around $10.8 \omega_0$), the same does not hold for $\rho(\omega)$ of CSIC clusters which behaves quite differently even for the largest cluster considered ($n=9$). This was illustrated by a superposition of $\rho(\omega)$ for CSIC and CSFCC $n=9$ clusters in panel denoted by $n=9$ in Fig. 3. Low frequency vibrations (up to about $8 \omega_0$) are quite similar in both types of sufficiently large clusters, but CSIC density of states does not exhibit characteristic features around $25 \omega_0$, which in a FCC crystal (bottom panel) are a consequence of the van Hove type of singularity related to features of dispersion of longitudinal and transversal modes (phonons) at the crystal Brillouin zone edges (see, e.g., Ref. 28).

The origin of the features around $10 \omega_0$ in CSIC and $10.6 \omega_0$ CSFCC clusters is in the large number of surface (poorly coordinated) atoms.¹⁵ Even for the largest cluster considered, made of 2869 atoms, 812 atoms are located at the cluster surface which makes about 28% (for smaller clusters the percentage is higher). This means that about 28% of the vibrational density of states represents the modes in which surface atoms are significantly displaced from their

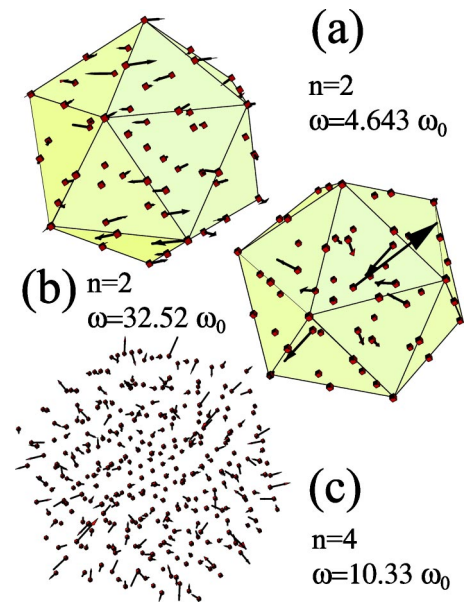


FIG. 4. Eigenvectors (displacement patterns) of three vibrational modes pertaining to CSIC clusters. The modes depicted in panels (a), (b), and (c) are those denoted by a, b, and c in Fig. 2, respectively. Equilibrium positions of cluster atoms are denoted by small cubes. The displacement vectors are multiplied by 10 in panels (a) and (b), and by 20 in panel (c).

equilibrium positions. Such modes are not present in the bulk crystal calculation. The peaks in $\rho(\omega)$ can in fact be related to the zone-edge frequencies of the Rayleigh-wave (RW) modes of surfaces of Lennard-Jones crystals.^{26,29} Additional confirmation of the identification of characteristic peaks can

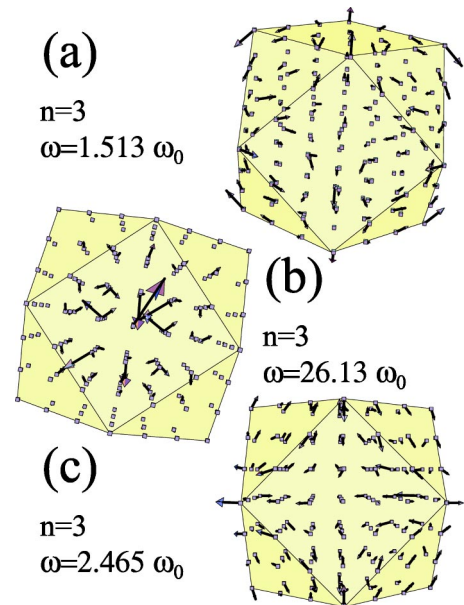


FIG. 5. Eigenvectors (displacement patterns) of some of the vibrational modes pertaining to CSFCC clusters. The modes depicted in panels (a), (b), and (c) are those denoted by a, b, and c in Fig. 3, respectively. Equilibrium positions of cluster atoms are denoted by small cubes. The displacement vectors are multiplied by 15 in panels (a), (b), (c).

TABLE II. Zero point energies (F_0) in units of $\hbar\sqrt{\epsilon/(M\sigma^2)}$ of Lennard-Jones icosahedral and cuboctahedral closed-shell clusters. The maximum cluster shell number is denoted by n .

n	Icosahedral, CSIC $F_0[\hbar\sqrt{\epsilon/(M\sigma^2)}]$	Cuboctahedral, CSFCC $F_0[\hbar\sqrt{\epsilon/(M\sigma^2)}]$
2	1018.571	
3	3083.370	3173.793
4	6854.732	7007.818
5	12787.93	13210.08
6	21138.61	22359.53
7	33097.20	34923.92
8	48960.54	51457.37
9	68577.49	72560.07

be found by inspecting panel (c) of Fig. 4 which displays the displacement pattern of a mode of $n=4$ CSIC cluster with a frequency of $10.33 \omega_0$. In this particular mode, mostly the surface atoms vibrate and the polarization vectors are oriented dominantly perpendicularly to the cluster surface. A similar pattern was found for larger CSIC and CSFCC clusters. However, the quality of the visual insight in the polarization pattern tends to degrade with the number of atoms in the cluster and this was the main reason for the choice of relatively small clusters for a visualization of the displacement patterns in Figs. 4 and 5 [see panel (c) in Fig. 4].

In Table II, the zero point energy,

$$F_0 = \frac{1}{2} \sum_{p=1}^{3N-6} \hbar\omega_p \quad (8)$$

pertaining to the CSFCC and CSIC clusters is presented. These results are to some extent surprising. Although both the minimum and maximum frequency are smaller in the CSFCC clusters, the first moments of their frequency spectra are *larger* than in corresponding CSIC clusters, at least for the cluster shell numbers between 2 and 9 studied here. One can visually inspect that this is indeed so by looking again at the panel denoted by $n=9$ in Fig. 3. This means that quantum ground state energies differ more than (classical) potential energies of the clusters. Thus, icosahedral closed shell clusters are even more preferred energetically when the quantum nature of the particles is important (in the cases when one can speak about the ordered ground state, when the approach presented here is adequate). To illustrate this effect and estimate its magnitude for clusters composed of rare gas atoms, in Fig. 6, I plotted the difference between the classical potential energies of CSIC and CSFCC clusters [$\Delta V_p^0 = V_p^0(\text{CSIC}) - V_p^0(\text{CSFCC})$, full circles] and the difference between the quantum ground state energies [$\Delta E_0 = V_p^0(\text{CSIC}) - V_p^0(\text{CSFCC}) + F_0(\text{CSIC}) - F_0(\text{CSFCC})$, empty diamonds] as a function of cluster shell number n , and for clusters composed of Ne, Ar, and Xe atoms. The insets in these plots display the values of ΔV_p^0 and ΔE_0 per cluster atom. These quantities cannot be obtained for general Lennard-Jones clusters in some reduced units of energy since the classical

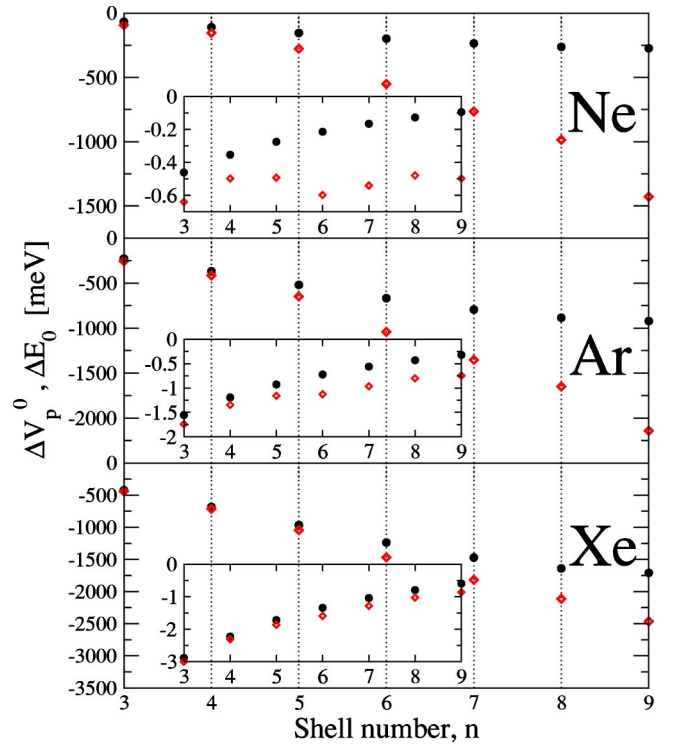


FIG. 6. The difference between the classical (full circles) and quantum (empty diamonds) ground state energies of CSIC and CSFCC clusters as a function of maximal shell number for Ne (top panel), Ar (middle panel), and Xe (bottom panel) clusters. The insets display the classical and quantum differences per cluster atom and as a function of shell number.

potential energy scales with ϵ , while the zero-point energy scales with $\hbar\omega_0$. The Lennard-Jones parameters used in this calculation were $\epsilon(\text{Ne})=3.07$ meV, $\sigma(\text{Ne})=2.75$ Å, $\epsilon(\text{Ar})=10.35$ meV, $\sigma(\text{Ar})=3.40$ Å, $\epsilon(\text{Xe})=19.18$ meV, $\sigma(\text{Xe})=4.1$ Å.³⁰ This produces characteristic frequency scales $\hbar\omega_0(\text{Ne})=0.29$ meV, $\hbar\omega_0(\text{Ar})=0.31$ meV, and $\hbar\omega_0(\text{Xe})$

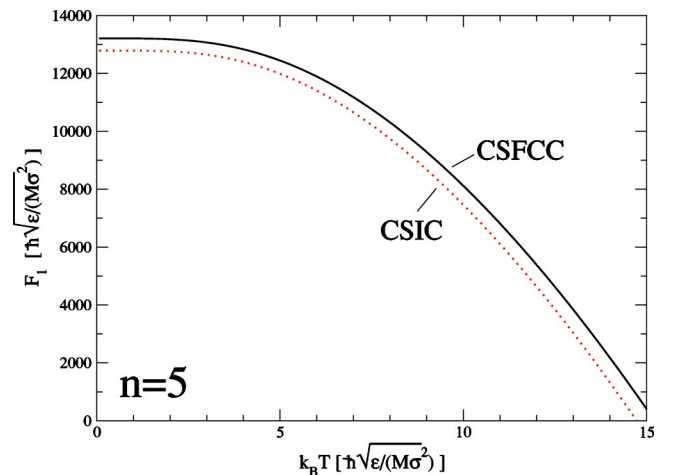


FIG. 7. Free energies of $n=5$ CSFCC (full line) and CSIC (dotted line) clusters measured from the corresponding classical potential energy minima [see Eq. (9)] as a function of reduced temperature $k_B T$.

=0.19 meV. The classical results (full circles) are practically the same as those obtained in Fig. 2 of Ref. 5. It is obvious that quantum corrections become more important for lighter atoms. Even for Xe clusters, their effect is not negligible, especially when the differences between the CSIC and CSFCC clusters are considered. Intriguingly enough, the relative importance of quantum effects does not uniformly decrease with the shell number. This is especially visible for Ne clusters (inset) where a significant “dip” in the quantum differences per cluster atom (ΔE_0) is obtained for $n=6$. The behavior of free energy with temperature is such that the differences between the CSIC and CSFCC free energies increase in absolute value as the temperature increases. This means that at finite temperatures, the CSIC structure is even more favored than at $T=0$ K. The behavior of the sum of second two terms in Eq. (4),

$$F_1 \equiv F - V_p^0 = \sum_{p=1}^{3N-6} \frac{\hbar\omega_p}{2} + k_B T \sum_{p=1}^{3N-6} \ln \left[1 - \exp\left(-\frac{\hbar\omega_p}{k_B T}\right) \right], \quad (9)$$

with temperature is illustrated in Fig. 7 for $n=5$ CSFCC (full line) and CSIC (dotted line) clusters. Similar behavior is found for all n 's examined in this work.

IV. SUMMARY AND CONCLUSION

The main result of this article is that quantal treatment of the low temperature properties of 3 to 9 shell CSIC and CSFCC Lennard-Jones clusters results in a larger binding energy of CSIC clusters. The difference between binding energies of CSIC and CSFCC clusters is larger than in classical treatment.⁵ This result is somewhat surprising in the view of expectations put forth in the Introduction. It is plausible, although not shown in this article, that the presented quantal treatment would yield a quantum binding energy “crossover” between the CSFCC and CSIC clusters for larger shell numbers than obtained classically (14), i.e., that the CSFCC arrangement of clusters would become energetically favorable for larger clusters than predicted previously.⁵ On the basis of Fig. 6 it can be expected that the exact number of atoms for which the crossover takes place is dependent on the mass of atoms in the cluster.

*Electronic address: asiber@ifs.hr

- ¹P. Moriarty, Rep. Prog. Phys. **64**, 297 (2001).
- ²J. J. Burton, J. Chem. Phys. **52**, 345 (1970).
- ³J. J. Burton, J. Chem. Phys. **57**, 1980 (1972).
- ⁴D. J. McGinty, J. Chem. Phys. **55**, 580 (1971).
- ⁵J. Xie, J. A. Northby, D. L. Freeman, and J. D. Doll, J. Chem. Phys. **91**, 612 (1989).
- ⁶J. A. Northby, J. Chem. Phys. **87**, 6166 (1987).
- ⁷B. W. van de Waal, J. Chem. Phys. **98**, 4904 (1993).
- ⁸J. P. K. Doye, D. J. Wales, and R. S. Berry, J. Chem. Phys. **103**, 4234 (1995).
- ⁹J. P. K. Doye and D. J. Wales, Chem. Phys. Lett. **247**, 339 (1995).
- ¹⁰B. W. van de Waal, Phys. Rev. Lett. **76**, 1083 (1996).
- ¹¹R. H. Leary and J. P. K. Doye, Phys. Rev. E **60**, R6320 (1999).
- ¹²F. Calvo, J. P. K. Doye, and D. J. Wales, J. Chem. Phys. **114**, 7312 (2001).
- ¹³H. S. Lim, C. K. Ong, and F. Ercolesi, Surf. Sci. **269/270**, 1109 (1992).
- ¹⁴J. P. K. Doye and D. J. Wales, J. Phys. B **29**, 4859 (1996).
- ¹⁵R. Meyer, L. J. Lewis, S. Prakash, and P. Entel, Phys. Rev. B **68**, 104303 (2003).
- ¹⁶F. Calvo and J. P. K. Doye, Phys. Rev. B **69**, 125414 (2004).
- ¹⁷W. Miehle, O. Kandler, T. Leisner, and O. Echt, J. Chem. Phys. **91**, 5940 (1989).
- ¹⁸S. Kakar, O. Björneholm, J. Weigelt, A. R. B. de Castro, L. Tröger, R. Frahm, T. Möller, A. Knop, and E. Rühl, Phys. Rev. Lett. **78**, 1675 (1997).
- ¹⁹C. Jayaprakash and W. F. Saam, Phys. Rev. B **30**, 3916 (1984).
- ²⁰K. R. Patton and M. R. Geller, Phys. Rev. B **67**, 155418 (2003).
- ²¹M. Born and K. Huang, *Dynamical Theory of Crystal Lattices* (Oxford University Press, Oxford, 1968).
- ²²H. Goldstein, *Classical Mechanics* (Addison-Wesley, Reading, 1980).
- ²³K. Huang, *Statistical Mechanics* (Wiley, New York, 1963).
- ²⁴D. Bressanini, M. Zavaglia, M. Mella, and G. Morosi, J. Chem. Phys. **112**, 717 (2000).
- ²⁵J. Uppenbrink and D. J. Wales, Chem. Phys. Lett. **190**, 447 (1992).
- ²⁶R. E. Allen, G. P. Alldredge, and F. W. de Wette, Phys. Rev. B **4**, 1648 (1971); **4**, 1661 (1971).
- ²⁷A. Šiber, Phys. Rev. B **66**, 235414 (2002).
- ²⁸N. P. Gupta and P. K. Garg, Solid State Commun. **16**, 607 (1975).
- ²⁹A. Šiber, B. Gumhalter, A. P. Graham, and J. P. Toennies, Phys. Rev. B **63**, 115411 (2001).
- ³⁰G. Stan, M. J. Bojan, S. Curtatolo, S. M. Gatica, and M. W. Cole, Phys. Rev. B **62**, 2173 (2000).